The Impact of Global Warming on Wind Power Potential in the Greater Horn of Africa

Bromwel Rhoda Apondi

Degree of Master of Science (120 credits)
with a major in Atmosphere, Climate and Ecosystems
60 hec

Department of Earth Sciences
University of Gothenburg
2023 B1258

Faculty of Science

UNIVERSITY OF GOTHENBURG

UNIVERSITY OF GOTHENBURG
Department of Earth Sciences
Geovetarcentrum/Earth Science Centre

The Impact of Global Warming on Wind Power Potential in the Greater Horn of Africa

Bromwel Rhoda Apondi

ISSN 1400-3821

B1258
Master of Science (120 credits) thesis
Göteborg 2023

Mailing address
Geovetarcentrum
S 405 30 Göteborg

Address
Geovetarcentrum
Guldhedsgatan 5A

Telephone
031-786 19 56

Geovetarcentrum
Göteborg University
S-405 30 Göteborg
SWEDEN

Abstract

The wind speed variability and wind power potential in the Greater Horn of Africa is analyzed in this study to fill a knowledge gap regarding if wind power can be used more as a source of energy for the region. This is investigated based on reanalysis data from ERA5, observed wind speeds, CORDEX-Africa regional climate models (RCMs) for future projections and a literature review. The study reveals a small but continuous increase in ERA5 wind speed with a significant correlation to the Indian Ocean Dipole (IOD) but this development is not well supported by the RCMs. The wind power potential was generally low upto the year 2100 but significant higher potential was seen in northern Kenya and Somalia, most likely due to the Turkana jet and the Somali jet. Despite the quantitative results, recommendations for further research regarding observation data and land cover changes in the region as well as uncertainties regarding the future warming of the Indian Ocean and its impact on the IOD are addressed as ways to improve the study as a strive for more robust results.

Keywords: Near-surface wind speed, the Greater Horn of Africa, ERA5, Wind power density, CORDEX-Africa

Acknowledgements

I would firstly like to thank my supervisor Deliang Chen for giving me the opportunity and the support to conduct this interesting and important study. Additionally, this study would have not been possible without the technical and theoretical support of Cheng Shen and for that, I am very grateful. Thank you to Grigory Nikulin at SMHI for the assistance with the CORDEX-Africa datasets as this was a important part of the project. To my fellow students, thank you for the great discussions and exchange of ideas during the course of this study.

Last but not least, thank you to my family and friends for the endless support and encouragement throughout this academic journey I have endured. None of this would have been possible without you.

Contents

1 Introduction

1.1 Motivation

As the global mean temperatures keep on rising and climate keeps on changing, different regions are directly or indirectly impacted in various ways. In effort to decarbonize to mitigate climate change, generation of renewable energy to reduce emissions is a a well-known strategy currently implimented. An example of renewable energy is using wind to generate wind power. For investments in wind power to be beneficial, understanding the possible outcomes of wind speed variability of a region is crucial.

$$P = \frac{\rho s f}{2} w^3 \tag{1}$$

The relationship between wind power(P)and wind speed(w) is according to Eq. (1) where ρ is the density, s is area covered by the turbine and f is an efficiency factor (Lu and McElroy (2017)).

Figure 1: The Greater Horn of Africa marked in green (Baudoin and Wolde-Georgis (2015)).

For this study, the Greater Horn of Africa was chosen for further understanding of wind speed variability and implications of wind power. This is a region in the eastern side of the African continent as Fig. 1 shows. It consists of the countries Sudan, South Sudan, Eritrea, Ethiopia, Djibouti, Somalia, Kenya, Uganda Rwanda, Burundi and Tanzania. The region also borders the Indian Ocean to the east and we can therefore say that it is confined within the coordinates 21°E and 52°E, 24.5°N and 12.5°S. Additionally, the region is undergoing rapid development in terms of population and the economical growth but has been assessed to be lagging in terms of sustainable energy (IEA (2022)). Therefore wind power could potentially be used as a supplementary source of renewable energy for the region.

1.2 Background

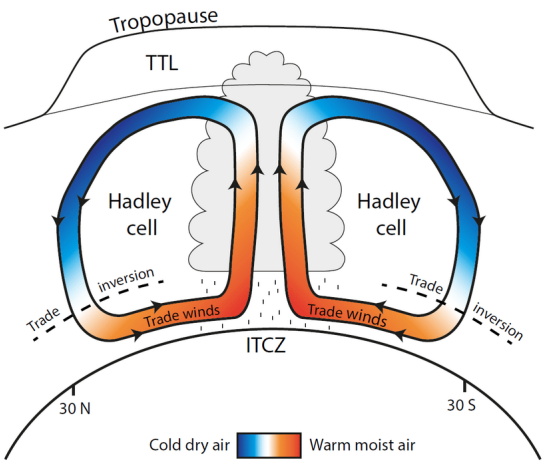

(a) An illustration of the Hadley cell (Fiehn (2017))

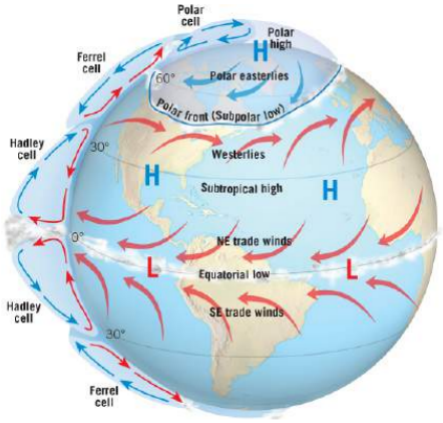

(b) Idealized global circulation for the three-cell circulation model on a rotating Earth (Lutgens (2018))

Figure 2

Since the study region is located in the tropics, it is predominantly warm as the region around the equator generally receives more solar energy than the rest of the globe. As a result, the relatively warm air rises and cools in the upper atmosphere, then heads polewards. Due to a rotation Earth, the air does not successfully reach the poles, but is instead deflected to the right in the Northern Hemisphere and to the left in the Southern Hemisphere with respect to the wind direction, due to the Coriolis force. At around 30°N and 30°S, the air descends and eventually heads back towards the equator. This circulation is well known as the Hadley cell (see Fig. 2(a)) and its lower parts result in the northeasterly (southeasterly) trade winds in the northern (southern) half of the tropics (see Fig. 2(b)). The trade winds converge around the equator in a zone known as the Intertropical Convergence Zone (ICTZ).

The ITCZ is mostly around the equator, but tends to follow the sun. Therefore it does shift northerly (southerly) during boreal summer (winter). Additionally, the shift is more prominent over land than over the ocean due to it having a greater heat capacity than land. Due to its convergence characteristics, ITCZ recognizable as a band of clouds with

enhanced convective precipitation. This is important in Greater Horn of Africa as the rain seasons depend on passage of ITCZ over the region.

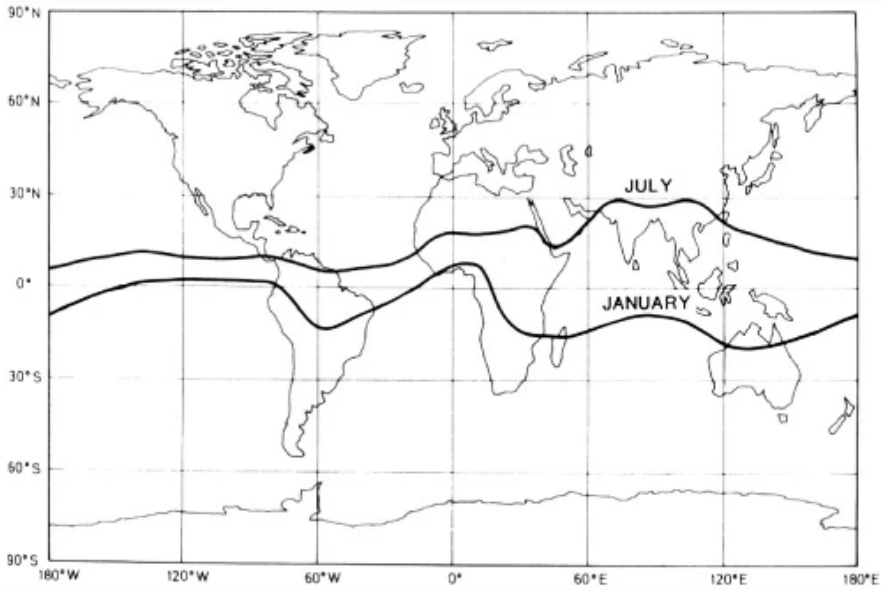

Figure 3: An illustration of the ITCZ during in June and January (Robinson and Henderson-Sellers (2014)).

In terms of the trade winds, the ITCZ also has the ability to shift wind directions depending on its positioning. This means that the south-easterly winds turn to be southwesterly when crossing the equator when the ITCZ is located to the north of the equator (Holton and Hakim (2013)).

$$Wind = PGF + CF + Fr \tag{2}$$

Eq. (2) is a simplified way of showing of the forces that are relevant for the resulting winds the study region. It shows that wind is a result of the balance between the pressure gradient force (PGF) due to pressure differences and the Coriolis force (CF) and friction (Fr) that is due to the surface roughness. The pressure gradient and surface roughness are the forces that directly impact the wind speed and the wind direction to some extent while the Coriolis force impacts the wind direction. The Coriolis force is proportional to the pressure gradient and its effect is therefore dependent on the wind speed. When further away from the surface of the Earth, the impact of the surface roughness on the wind decreases.

In the northern hemisphere, there has been a decrease in the mean near-surface wind speeds until 2010, a phenomenon referred to as stilling. Thereafter a reversal of the mean near-surface wind speeds in the northern hemisphere is detected. This stilling and reversal is shown to regionally be highly correlated to inter-decadal ocean-atmosphere os-

cillations such as the NAO for Europe, the PDO for Asia and the TNA for North America (Zeng et al. (2019)). Zeng et al. (2019) also argue that the surface roughness (land cover changes) did not suddenly shift at 2010, leaving the development in observed near-surface wind speeds to be mainly dependent on ocean-atmosphere oscillations. The Indian Ocean is another water-body that could potentially have an impact on the terrestrial winds of the regions around its basin, which includes the Greater Horn of Africa. Saji et al. (1999) showed that there is an ocean-atmosphere interaction over the Indian Ocean, which is referred to as the Indian Ocean Dipole (IOD) in this study, that does not depend on the El Niño–Southern Oscillation (ENSO). The intensity of the IOD is determined by the sea surface temperature SST) gradient across the Indian Ocean basin (between the western equatorial Indian Ocean (50E-70E and 10S-10N) and the south eastern equatorial Indian Ocean (90E-110E and 10S-0N)). This temperature difference is then translated to the Dipole Mode Index (DMI) and the greater the temperature gradient, the more intense the IOD event is.

(a) Positive IOD

(b) Negative IOD

Figure 4: The positive and negative phases of the Indian Ocean Dipole and their respective precipitation patterns (NOAA (2020a), NOAA (2020b)).

Depending on where along the equatorial Indian Ocean the sea surface is warmer or cooler than average, the DMI can be negative or positive. When DMI is positive (negative) then the phenomenon is referred to as a positive (negative) IOD event. In a positive IOD event, the SST is higher than average over the western Indian ocean while it is lower than average in the east/southeast as Fig. 4(a) shows. This creates a temperature (pressure) gradient, creating a flow westwards and convergence around the East African coast, leading to enhanced rainfall in the region. On the eastern end of the ocean, a cooler than

average sea and descending air results in drier conditions over Southeast Asia and Australia. Fig. 4(b) shows a negative IOD event, which results in drier conditions in the western and wetter conditions in the eastern parts of the Indian ocean. This dipole has therefore shown an impact on precipitation patterns over the regions around the Indian Ocean basin as well as the surface winds over the ocean, mainly its zonal component (Saji et al. (1999)).

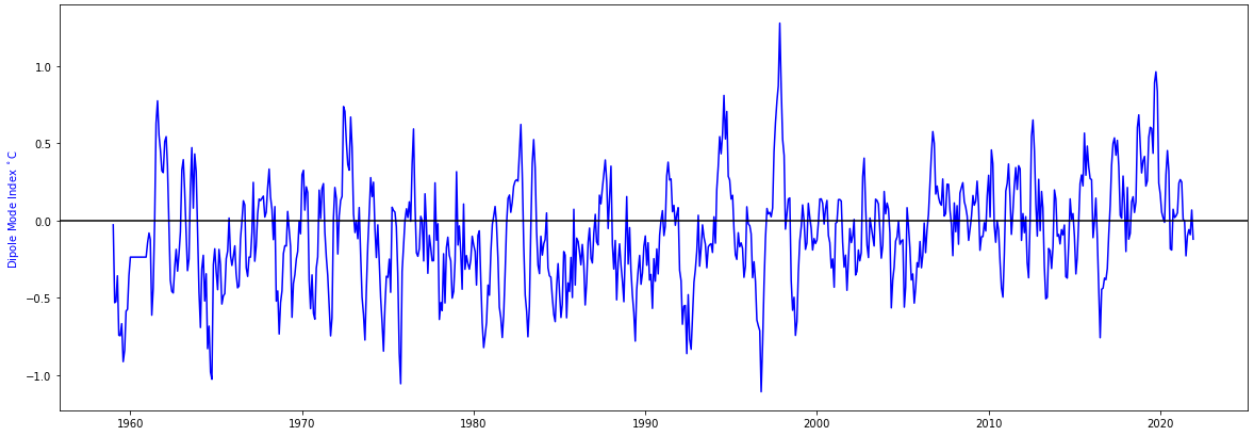

Figure 5: The Dipole Mode Index showing years with positive and negative Indian Ocean Dipole events during the time period 1959-2021.

Previous studies such as Black et al. (2003), Saji and Yamagata (2003b) and Behera et al. (2003) have mainly focused the impact of IOD on rainfall anomalies over East Africa. From looking at Fig. 5, There have been various positive and negative IOD events in the past decades. An example is the year 1997 when there was a strong positive IOD event that Webster et al. (1999) showed resulted in heavy rainfall in East Africa. There have also been studies of regional climate models satisfactorily simulating rainfall in East Africa when using their ensemble mean (Endris et al. (2013)). In terms of winds, there are significantly less studies and the studies that are available focus mostly on the wind zonal variability over the ocean as Saji and Yamagata (2003a) and Webster et al. (1999) showed.

In terms of wind power potential, there are a few studies that have been conducted based on the CORDEX Africa Regional Climate Models. Based on the CORDEX-CORE ensemble, Sawadogo et al. (2021) showed that the Horn of Africa was one of the regions that showed a high wind power potential under global warming and therefore advantage-

ous in terms of wind power investments in the present (2021-2040) climate and in the mid century (2041-2060). Not too far from this thesis's study area, Libanda (2022) conducted an assessment of how well 12 CORDEX regional climate models (RCMs) simulate wind speeds over Zambia while using the reanalysis data ERA5 as the reference data set but no observational data for verification. The study showed that the RCMs were able to reproduce the wind speeds' annual cycle and geographical patterns. with varying magnitude. Of all the RCMs, the study suggests that an ensemble mean of the three best performing models (RCA4-GFDL-ESM2M, RCA4-HadGEM2, and RCA4-CM5A-MR) would give the best estimate for the future wind power potential in Zambia.

There are clearly not many studies regarding terrestrial wind speed variability and spatial patterns in the Greater Horn of Africa but this is crucial information as it is a parameter that significantly determines the wind power potential of the area. Finding potential correlations to other ocean-atmosphere oscillations could also be key in the prediction of future wind speeds. Therefore this study fills a knowledge gap regarding wind speed variability historically, currently and in the future and its direct impact on wind power potential in the Greater Horn of Africa.

1.3 Objective

To understand the wind power potential over the Greater Horn of Africa, the study analyzes the past and future wind speed changes in this region under global warming. This would also contribute to the lack of studies regarding winds in this region. Three research questions are addressed to conduct this study:

- How has the wind speed changed during the past decades over the Greater Horn of Africa?
- How are the wind speeds expected to change in this region under global warming?
- What does the estimated wind speeds indicate in regard to the wind power potential in this region?

This thesis is divided into several sections to provide the reader with necessary understandings about wind speed variability and analysis of wind speed data. As seen in Section 1.1, the atmospheric conditions and some previous studies are presented to get a deeper understanding of what factors are affecting wind variations in the Greater Horn of Africa. The methodology of the study is briefly explained in Section 2, since the datasets used and the steps taken were crucial implements of this research and laid the foundation for the analysis. The results from the analysis are presented in Section 3 and the study ends in a discussion in Section 4 and a conclusion in section 5, where also possible future research is brought to attention.

2 Methodology

2.1 Datasets

For the research questions to be answered, different data sets from different sources were analyzed. Firstly, observation dataset with an hourly time resolution were attained from HadISD by the Met Office Hadley Center (Dunn et al. (2012), Dunn et al. (2016), Dunn (2019)). For the daily mean to be calculated, a criteria was set that each day had to have at least two valid value rates. Thereafter, the monthly mean was calculated with the criteria that each month had to have at least 50% of the valid value rates. This led to 21 stations with 10m wind speed observations from 1980 to 2021 being found within the defined region, which consequently included stations in the Middle East and Northern Africa (outside the Greater Horn of Africa) that were excluded moving forward. Due to the varying lack of data from the remaining stations, the following criteria were implemented as an attempt to filter out the data that could have a significant impact on the results. Firstly, only stations that had over 90% of the total data were used as the majority of the stations (10 out of 17) did pass this criteria. Since the observational data was to be quantitatively compared with a reanalysis dataset (ERA5), this step was an attempt to make these different datasets as comparable as possibly. Qualitatively, this step does not guarantee that observation stations with over 90% of the total wind speed data that could have been observed

are better than those with lower than 90% as other factors such as how the measurements are conducted, topography and infrastructure around the measurement stations cannot be easily excluded/filtered out. Therefore, there is a risk in such filtering as it does not guarantee better quality of the remaining data even though in this study, it is assumed to be beneficial for quantitative analysis. Secondly, coastal stations were excluded since local phenomena such as sea-breeze have an impact on the wind speeds (and direction).

Figure 6: A map of Kenya with the location of the stations (red dots) providing the data used in this study.

This procedure led to observational data from 8 stations only were used in this study and all of them were located in Kenya (see Fig. 6). The annual mean of the wind speed

from the chosen stations was calculated and compared to the annual mean of the wind speed of ERA5 grid point closest to the location of each respective observation station.

Due to the lack of enough coverage of wind observation in the study region, ERA5, a global reanalysis dataset was used to understand the historical development. ERA5 is a state-of-the-art reanalysis dataset developed by the European Centre for Medium-Range Weather Forecasts (ECMWF). It provides comprehensive information about the Earth's atmosphere, land surface, and ocean variables with global coverage and high spatiotemporal resolution. The dataset assimilates a wide range of observational data in combination with a numerical weather prediction model to generate a more consistent approximation of the past weather conditions. The ERA5 dataset shows an improvement in terms of temperature, wind, and humidity in the troposphere (but not in the stratosphere) in comparison to its predecessor ERA-Interim. This gives reanalysis datasets an advantage in the study region due to better resolution and better coverage in comparison to the available observational data. However, 10 m wind observations over land is a type of in-situ data that is not assimilated in ERA5. The exclusion of 10 m wind observations over land could be due to the non-guaranteed quality and homogeneity of surface wind measurements. As mentioned earlier, 10 m winds can also be impacted by other factors such as topography and infrastructure, which contributes with biases and inconsistencies in terms of the estimated wind fields. To address this, reanalysis datasets like ERA5 rely on parametrization to reasonably estimate 10 m winds over land by using a combination of surface and atmospheric characteristics and other related parameters based on the availability (Hersbach et al. (2020), Dee et al. (2011)). The 100 m winds from ERA5 reanalysis were also used in this study. There are several other reanalysis datasets that could be used but in this case ERA5 was chosen highly due to a previous study that showed that it was in best agreement with observed wind speeds and variability out of five state-of-the-art global reanalyses (Ramon et al. (2019)).

As mentioned earlier, changes ocean-atmosphere oscillations have shown to most likely be a determining factor in near surface wind changes (Zeng et al. (2019)). Taking this into consideration as well as the geographical positioning of the study region, the Indian Ocean potentially having an impact on the terrestrial winds was taken into account. As

shown by Saji et al. (1999), the Indian Ocean Dipole that is determined by the sea surface temperature gradient between the western and eastern tropical Indian Ocean does have an impact in the climate variability in the surrounding regions, including East Africa. A dataset containing the monthly Indian Ocean Dipole Index was attained from the National Oceanic and Atmospheric Administration for analysis (NOAA (n.d.)).

For a better understanding of the performance of climate models as well as the impact of global warming on the wind speeds in the study area, datasets provided by CORDEX (Coordinated Regional Climate Downscaling Experiment) were attained via the database https://esgf-data.dkrz.de/search/cordex-dkrz/. Since CORDEX focuses on regional climate downscaling, CORDEX-Africa was used as it had several regional climate models (RCMs) covering the study region that provide the parameter wind speed. Furthermore, the regional models that currently have the highest resolution of 0.22°x0.22° in the African domain were used (also known as AFR-22). This was better fitting for this study to better capture finer details within the study region such as the impact of topography. For the 10m wind speed, three RCMs in AFR-22 were used; CLMcom-KIT-CCLM5-0-15, GERICS-REMO2015 and ICTP-RegCM4-7. These RCMs are driven by three historical Coupled Model Intercomparison Project Phase 5 (CMIP5) global climate models (GCMs) respectively; MOHC-HadGEM2-ES, MPI-M-MPI-ESM-LR and NCC-NorESM1-M. This means that the GCMs driving the RCMs have been run backward in time to acquire their historical climate circumstances that could be compared with other datasets such as reanalysis data as well as forward in time under two RCP scenarios; RCP 2.6 and RCP 8.5. Datasets consisting of the u and v components of 100 m winds were also used, which is currently solely in the regional model ICTP-RegCM4-7 (CORDEX (2022)). For all datasets acquired from CORDEX-Africa, there were divided into two parts; the first part is the historical simulation which is from 1950 or 1970 to 2005 and the second part was the simulation of RCP 2.6 and RCP 8.5 which are up to 2100.

2.2 Procedure of analysis

For the analysis and illustration of the data, the programming language Python was used. Additionally, the software program Climate Data Operator (CDO) was used as it facilitates

the processing of climate data (Schulzweida (2017)). For all datasets, the region of study was defined within the coordinates 21°E and 52°E, 24.5°N and 12.5°S. Thereafter, the data points over the ocean were masked out as the study's point of interest was winds over land. This was particularly important as part of the Indian Ocean that is included in the define region was assumed to have a significant impact on the results. Thereafter, yearly mean was derived for all the data sets and a moving average with a window size of 10 years was applied. The calculation of the yearly mean was used to reduce noise in the dataset since the monthly data has larger variability which made the detection of trends in a longer time scale more complex. Having a moving average with a window size set to a decade was also a way to detect potential interannual variability that was clearly shown in other regions of the northern hemisphere by Zeng et al. (2019). Furthermore, the seasonal mean of some of the datasets were also calculated to see if the variability of the wind speed was impacted by the time of the year. The seasons were defined as December to February, March to May, June to August and September to November. After the seasonal grouping was attained, the 10-year moving average was applied in the same manner as it was for the yearly mean.

To detect and visualize the changes in the wind speed, a simple linear regression as Eq. (3) shows was used.

$$y = ax + b \tag{3}$$

In this study, y was the wind speed that depends on the time which in this equation can be considered as x. The slope a was the trend of wind speeds during the defined time period, which at times varied per dataset, and was formulated in the units m/s per decade. Lastly, b is a constant in Eq. (3).

When comparing the development in data sets, the correlation coefficient was used to determine if there was a correlation between the 10 year moving averages of the wind speed and the IOD. Due to the datasets being For this study, the Pearson correlation coefficient(r) was calculated based on Eq. (4) where x_i is values of the x-variable in a sample, $\bar{x}$ is the mean of the values of the x-variable, y_i is values of the y-variable in a sample and $\bar{y}$ is the mean of the values of the y-variable.

$$r = \frac{\sum_{i=1}^{n}(x_i - \bar{x})(y_i - \bar{y})}{\sqrt{\sum_{i=1}^{n}(x_i - \bar{x})^2}\sqrt{\sum_{i=1}^{n}(y_i - \bar{y})^2}} \tag{4}$$

The Pearson correlation coefficient can also be used to conduct a significance test with a resulting p-value. The level of significance within the hypothesis test was set to 0.05. Therefore, if the p-value was less than 0.05 then the acquired results were considered statistically significant, thus the null hypothesis could be rejected.

$$WPD = \frac{\rho w^3}{2} \tag{5}$$

To determine the wind power potential, the wind power density (WPD) was calculated using Eq. (5) where ρ is the air density and w is the wind speed. For simplicity, ρ was assumed to be 1 kg/m^3.

3 Results

3.1 Observed wind speeds

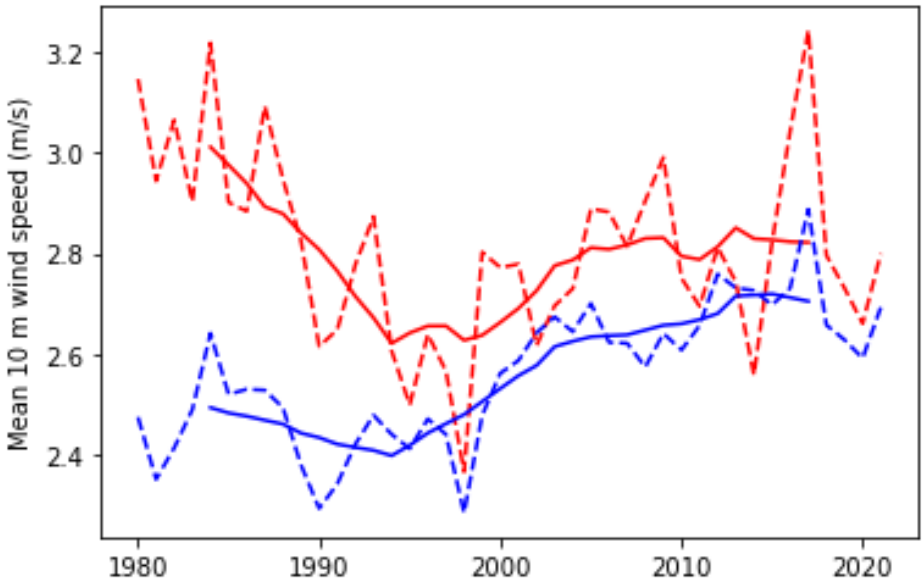

Figure 7: The mean annual 10m mean wind speed from 8 observation stations in Kenya (red dashed line) its 10-year moving average (red line) as well as the respective ERA5 10 m mean annual wind speed (blue dashed line) and its 10-year moving average (blue line).

As mentioned earlier, there is a lack of wind observations in the Greater Horn of Africa. The observational data that was found was analyzed for additional verification to the reanalysis dataset ERA5. Fig. 7 shows the annual mean and the 10-year moving average of the observed wind speed in Kenya from 8 different stations. Additionally, ERA5 was used for comparison which shows that in the 80s and most of the 90s, ERA5 underestimates the wind speeds somewhat, despite similar development as seen in the observations throughout 1980 to 2021. Approximately from the year 2000 and onward, the difference between the ERA5 wind speeds and the observed wind speeds is smaller. Further details such as the topography within a relevant diameter from the stations or the standard of the observation stations were not investigated further which could also play roll in the development seen in the observations in Fig. 7.

3.2 An increase in ERA5 winds speeds and a correlation to the Indian Ocean Dipole Index

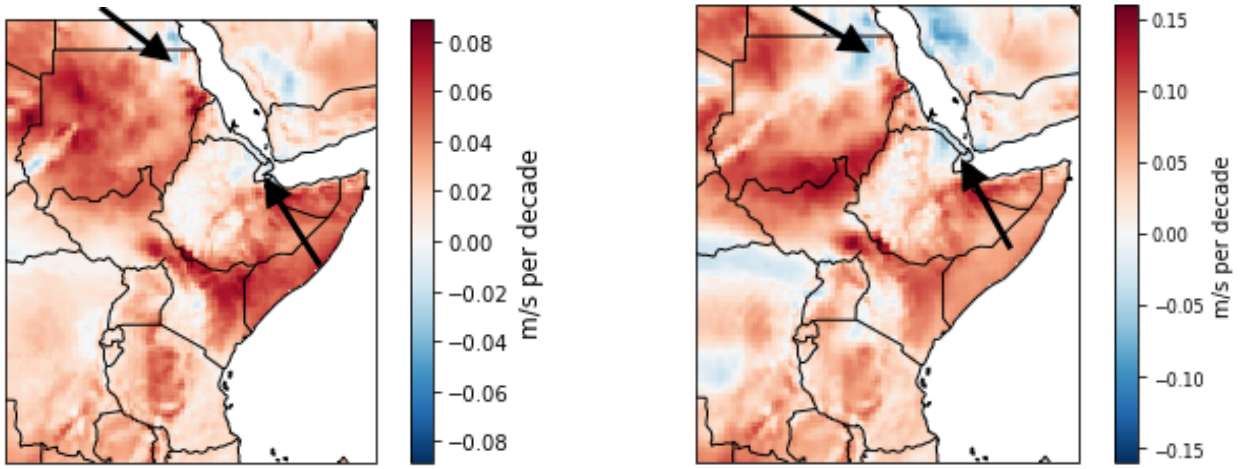

(a) 10m wind speed

(b) 100m wind speed

Figure 8: The trend of the ERA5 annual a)10 m and b) 100 m mean wind speed for 1959-2021. The black arrows indicate the regions where a decrease in wind speed is detected.

Looking into the ERA5 datasets, Fig. 8 shows where the greatest changes in 10 m and 100 m wind speeds have occurred in the study region during the time period 1959-2021. Most of the region tend so show an increase in the wind speeds but some slight decrease in wind speed is detected in northern and north-eastern Sudan, northern Ethiopia, Eritrea and Djibouti, pointed by the black arrows in Fig. 8.

Fig. 9 show a continuous increase in wind speeds over the Greater Horn of Africa during the time period 1959-2021. For the 10 m and 100 m wind speeds, the mean increase is 0.028 m/s and 0.043 m/s per decade respectively but as Fig. 8 shows, this varies spatially. When the IOD index's 10-year moving average was incorporated, it showed that it has a significant positive correlation to both the 10m and 100m wind speeds with the correlation coefficient 0.85 and 0.77 respectively. The performance of a significance test of the concluded correlation between the wind speeds and the IOD index returned a p-value below the significance level of 0.05.

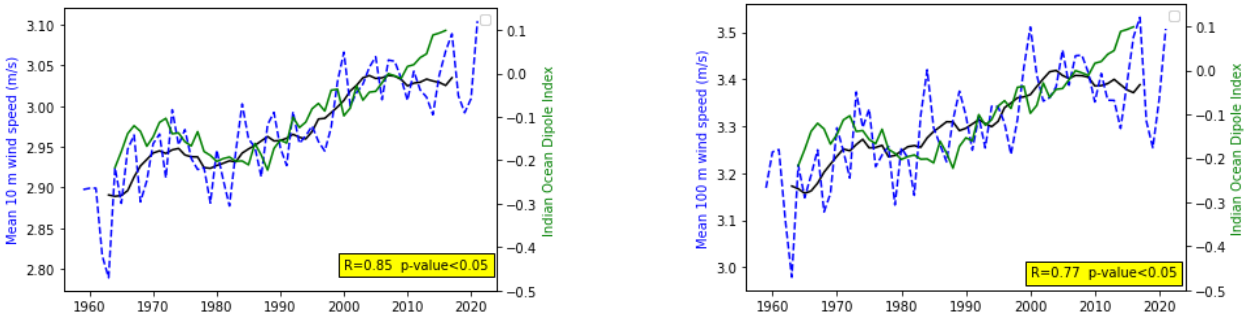

(a) 10 m wind speed

(b) 100 m wind speed

Figure 9: The ERA5 annual a)10 m and b)100 m mean wind speed (blue dashed line) and its 10-year moving average (black line) as well as the 10-year moving average of the Indian Ocean Dipole (green line) for the time period 1959-2021.

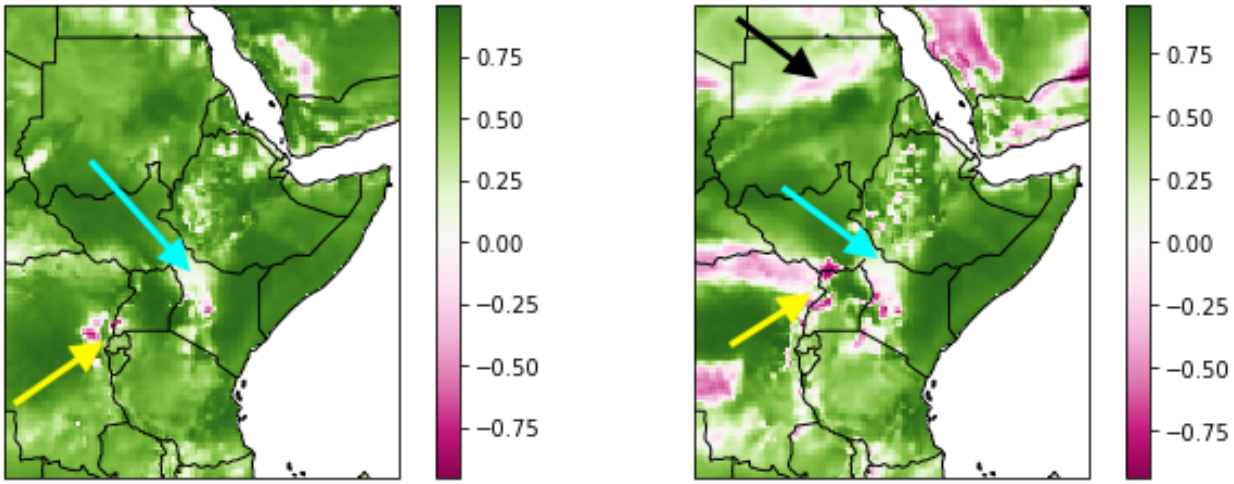

(a) Correlation 10 m wind speed

(b) Correlation 100 m wind speed

Figure 10: The correlation coefficient between the 10-year moving average of the Indian Ocean Dipole and the ERA5 a) 10m wind speed and b)100 m wind speed for the time period 1959-2021.The blue arrow shows the region in Kenya with mostly no correlation and the yellow arrow shows the study region's border to the Democratic Republic of Congo with a negative correlation.

To further determine the significance of the correlation of wind speeds over the Greater Horn of Africa and the Indian Ocean Dipole, the spatial variability of the correlation coef-

ficient is shown in Fig.10. The figures how that the decennial average 10m and 100 m wind speed have a significant positive correlation to the IOD for most of the study region. Fig.10 also shows that there is less correlation in smaller parts of Kenya (marked by the blue arrow) and in the area where the study region borders the Democratic Republic of the Congo (marked by the yellow arrow). For the 100m wind speeds, there is less correlation to the IOD in parts of northern Sudan as well (marked by the black arrow in Fig.10(b).

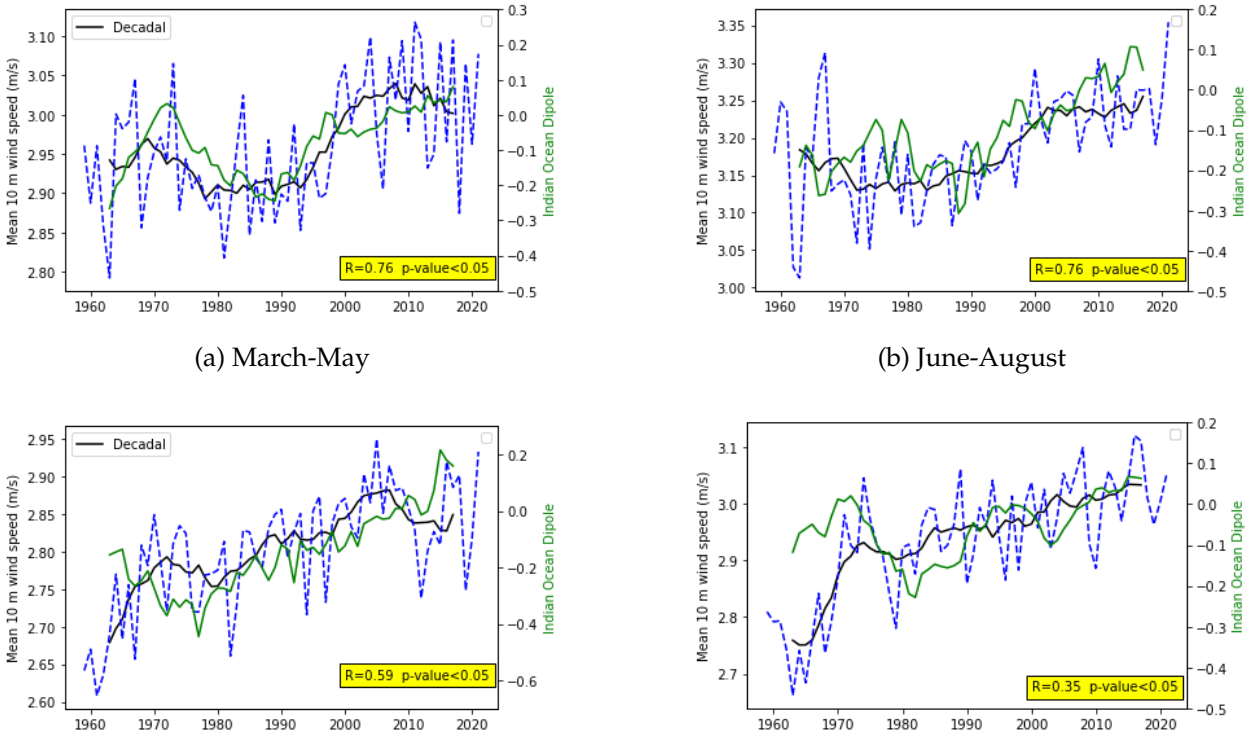

(a) March-May

(b) June-August

(c) September-November

(d) December-February

Figure 11: The ERA5 seasonal 10 m mean wind speed (blue dashed line) and its 10-year moving average (black line) as well as the 10-year moving average of the Indian Ocean Dipole(green line) for the time period 1959-2021.

A similar analysis was performed for the seasonal 10 m wind speeds as well since the Indian Ocean Dipole cycle does vary during the year. It is known to start some time during boreal spring and diminish approximately towards the end of boreal autumn (Saji et al. (1999)). Based on Fig. 11, the wind speeds and the IOD has the weakest correlation during boreal winter with a correlation coefficient of 0.35. The correlation to the IOD

index is significantly higher during boreal spring and summer with both seasons having a correlation coefficient of 0.76.

3.3 CORDEX-Africa historical wind speeds

3.3.1 *Historical 10 m wind speeds of regional climate models*

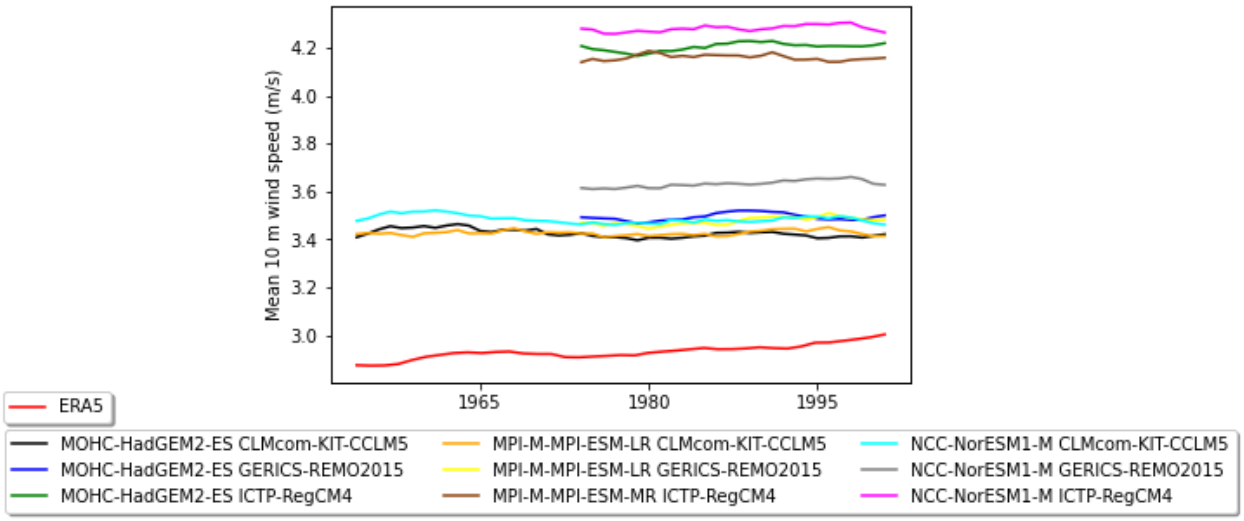

Figure 12: The 10 m wind speed 10-year moving averages of the 10 m wind speed in ERA5 and the RCMs covering the Greater Horn of Africa for the time period 1950-2005.

Looking at the historical 10 m wind speeds in three regional climate models downscaled from three global climate models, Fig.12 shows the differences between the 10-year moving average in the models and the ERA5 data set. It is clear that all the RCMs overestimate the wind speeds in comparison to ERA5. Despite this, there is no significant increase or decrease in the 10-year moving average of the wind speeds in the RCMs but a slight increasing trend is seen in ERA5. The significance of the changes in wind speeds is also seen Fig.13 that shows the different RCMs for the time period 1950-2005. The changes in wind speed are small for all RCMs and they do not tend to agree on where the the greatest increase or decrease has occurred during the time period.

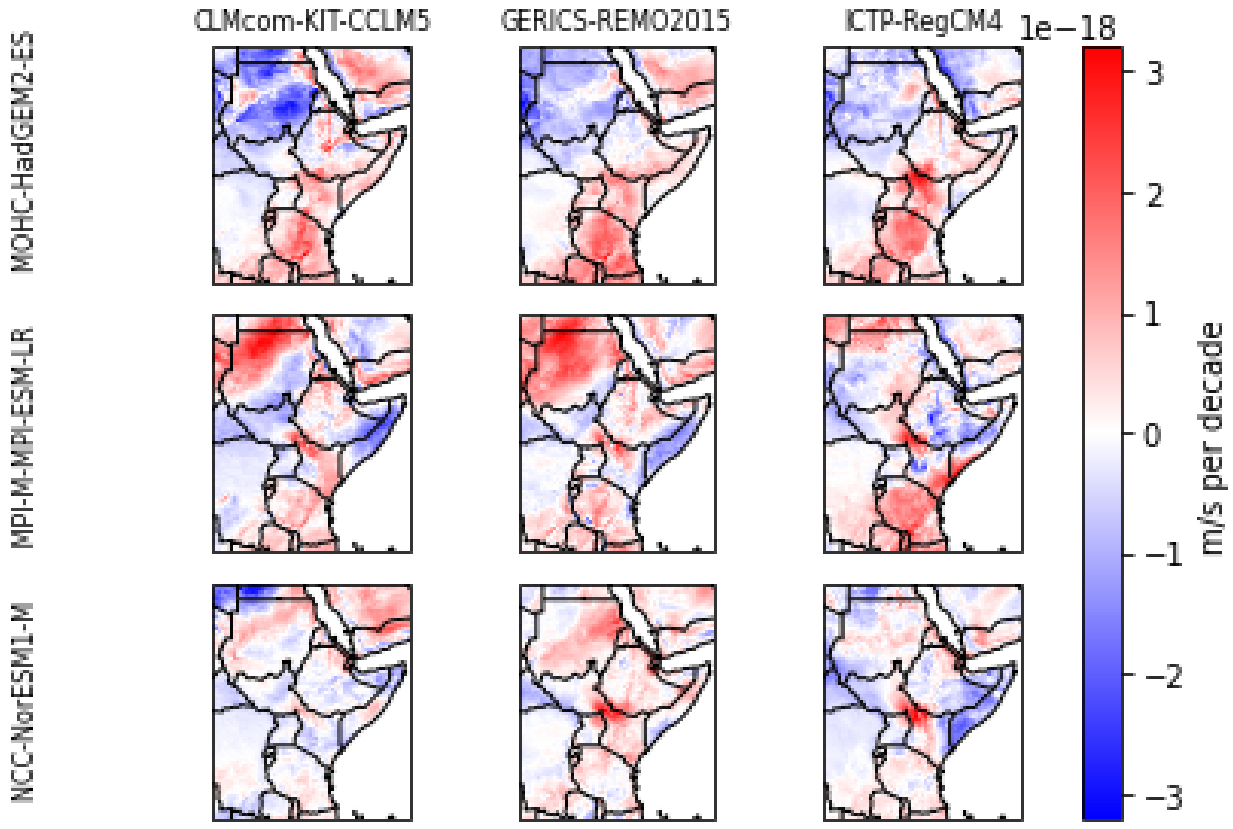

Figure 13: The trend of the annul mean wind speed in RCMs for the time period 1970-2005.

3.3.2 *Historical 100 m wind speeds of regional climate models*

In a similar manner, the historical 100 m wind speeds in three RCMs based on a downscaling of one global climate model were analyzed. Fig. 14 also shows that the RCMs overestimate the wind speeds in comparison to ERA5 and the overall changes in the decennial wind speed are rather small. ERA5 is also the only one that seems to be showing a distinctive increase in wind speeds. Similarly to the 10 m wind speeds, the changes in the 100 m wind speeds are small as Fig.15 shows. Fig.15 also supports an overall increase in wind speeds in the study region in ERA5 than the RCMs.

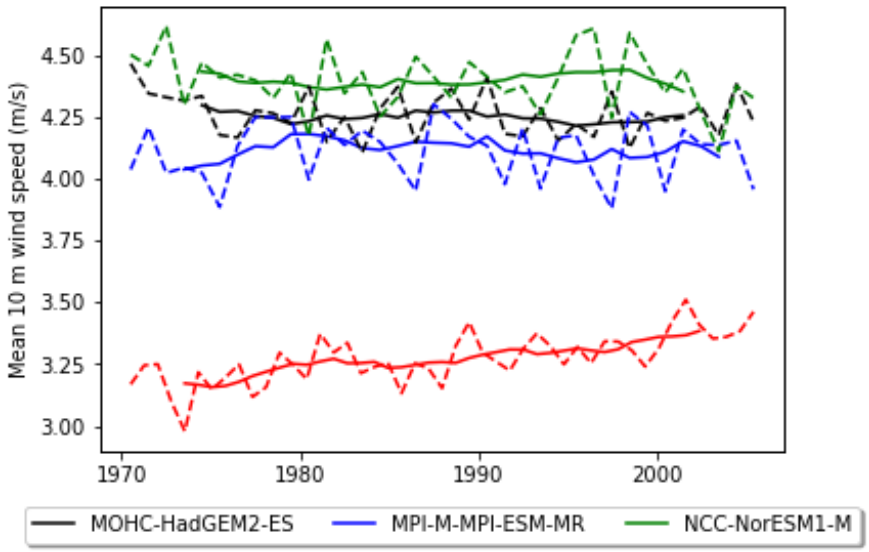

Figure 14: The 100 m wind speed 10-year moving averages in ERA5 and the RCMs covering the Greater Horn of Africa.

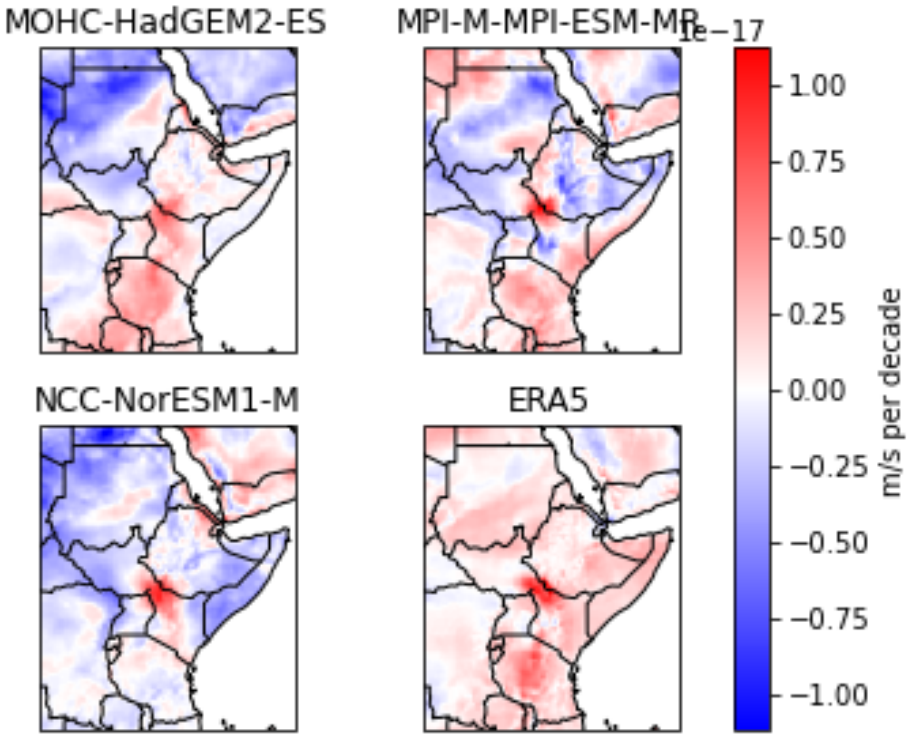

Figure 15: The trend of mean 100 m wind speed for the time period 1970-2005 in the respective RCMs and ERA5.

3.3.3 *Future wind speed projection*

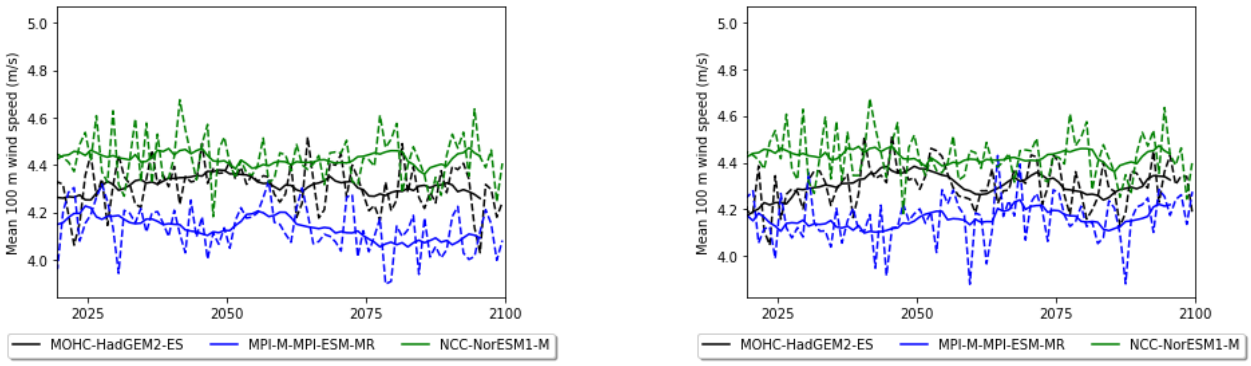

(a) RCP 2.6

(b) RCP 8.5

Figure 16: The 100 m mean wind speed for the time period 2024-2100 in the respective RCMs for a) RCP 2.6 and b) RCP 8.5.

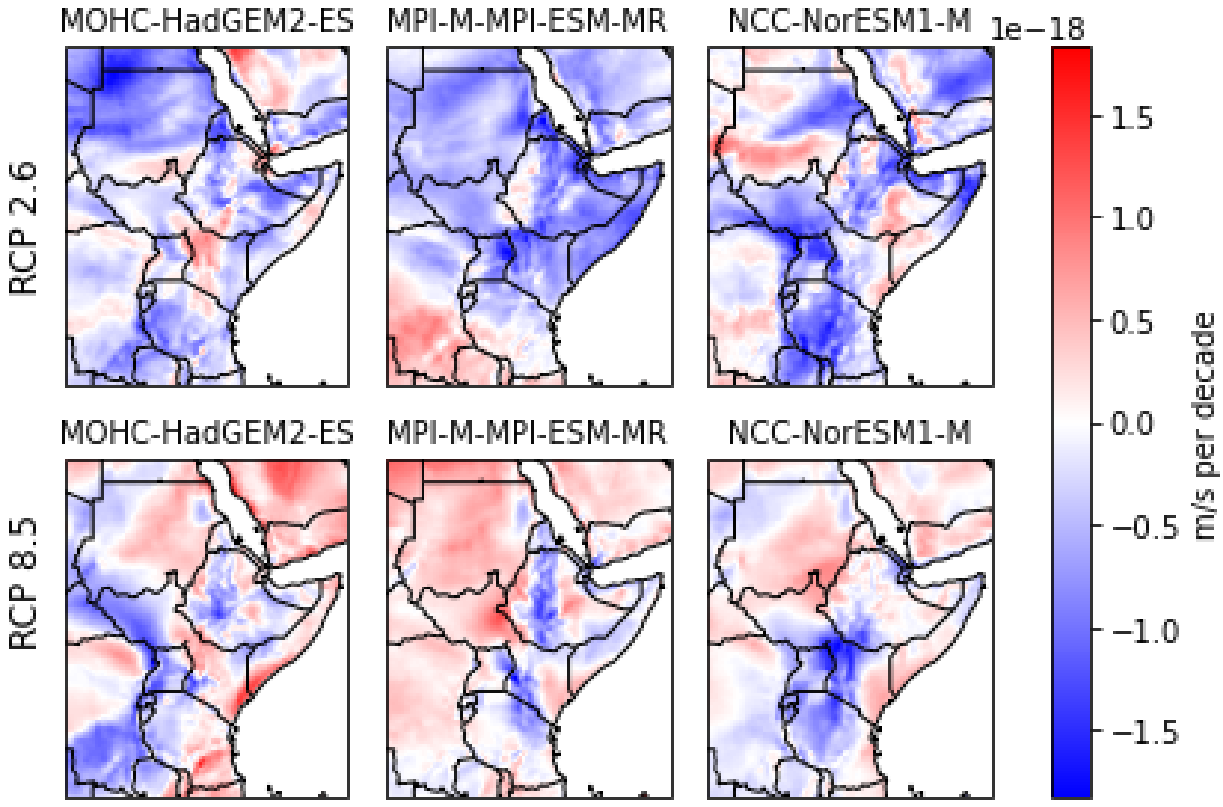

Figure 17: The trend of 100 m wind speed for the time period 2024-2100 in the respective RCMs for RCP 2.6 and RCP 8.5.

In order to estimate the wind power potential for the Greater Horn of Africa, a future projection of the 100 m wind speed was analyzed. Under global warming, the RCMs show that the mean 100 m wind speeds in the study region do not change significantly for both RCP 2.6 and RCP 8.5 as Fig. 16 illustrates. Looking further into the spatial variability, Fig.17 illustrates that there are tendencies of increasing wind speeds in a warmer global climate, which is seen in RCP 8.5 than in RCP 2.6. Despite the differences, the projected mean wind speed changes in the study area are rather small.

3.4 Wind power potential

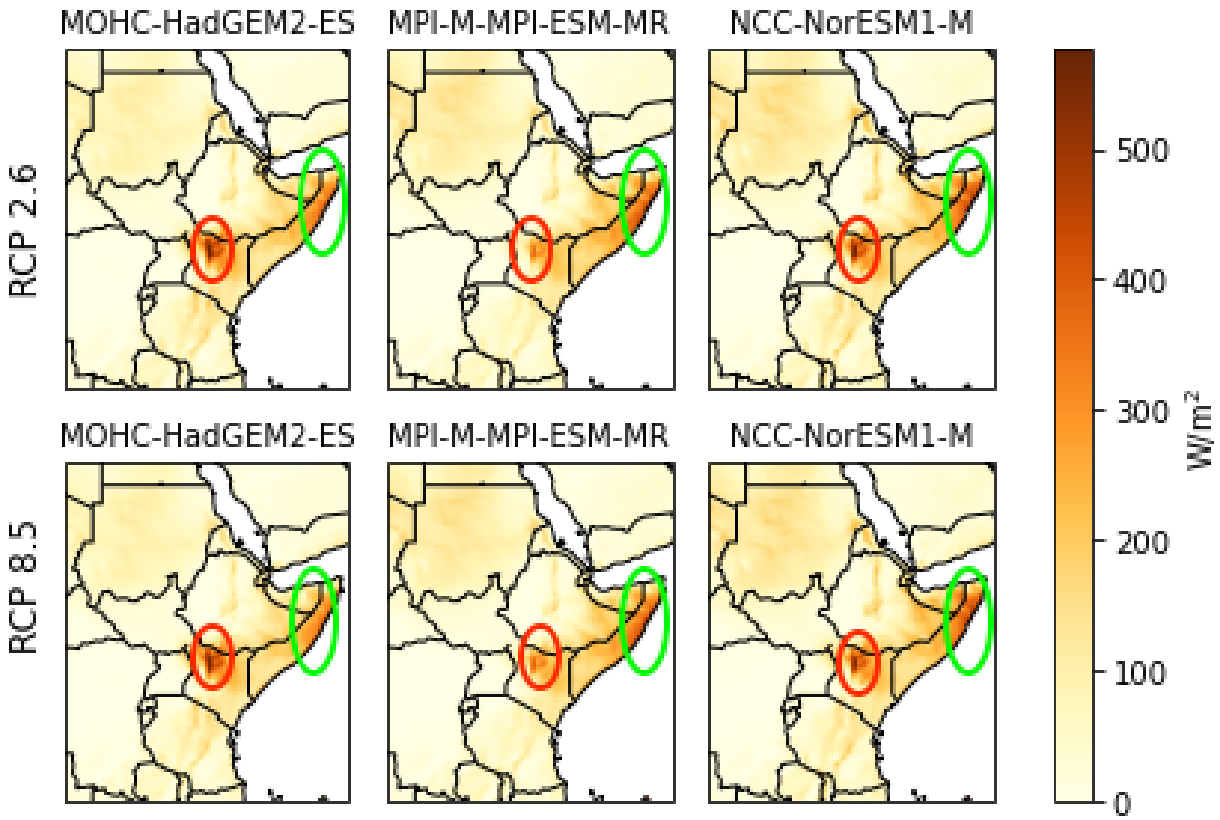

Figure 18: The wind power potential for the time period 2024-2100 in the respective RCMs for RCP 2.6 and RCP 8.5. The regions with the highest wind power potential are in northern Kenya (red oval) and parts of Somalia (green oval).

Based on the 100 m projected wind speeds under global warming, a mean of the wind speeds over time was used to determine the wind power potential (WPD). Similarly to the minor changes of the wind speeds in the study region under global warning, the WPD is not expected to change much. Fig. 18 shows that the WPD is quite low for most parts of the study area. It also shows that in parts of Somalia and northern Kenya are the areas within the study region where the highest WPD is detected.

4 Discussion

This study shows that there is in general no high 10m or 100 m mean wind speeds and the differences in the past and coming decades are rather small. Despite these results, discussion points regarding the wind speed observations in the region, potential land cover changes, areas with higher wind power potential and uncertainties regarding the Indian Ocean warming are addressed below as they play a roll in the wind speed development in the Greater Horn of Africa.

4.1 A need for more observation data for verification

Looking at the winds in the past decades (1959-2021) based on ERA5 reanalysis data, there is a continuous increase of wind speeds in the Greater Horn of Africa. The lack of widespread wind observations in the region for verification makes the increase of wind speed detected in this study less reliable. However, Fig. 7 does in some way verify that the wind speeds in ERA5 could act as a good estimate to compensate for the lack of observations. It is important to note that this verification is rather limited and could be more robust if there were more stations measuring wind spread out in the study region. Additionally, the filtering process that was described in Section 2.1 could also have an impact on the results in terms of quality, as well as the location of the stations with respect to the terrain, which Fig. 6 partly shows. Apart from ERA5, there are other reanalysis data sets could and should be analyzed for further understanding of the wind speed variability as a strive for robustness in wind speed changes in different datasets.

As we know from Section 1.1, there wind speed does highly depend on the pressure

gradient. An alternative of understanding the wind speed variance over time could be to use barometric pressure observations. From this, the pressure gradient force could be derived and as Eq. (2) showed, the resulting wind speed is highly dependent on it. For wind power potential, the exact wind speed values are not of as much importance as the magnitude of change observed, which gives room for other relevant parameters to be able to give this information where wind observation data is lacking.

Using remote sensing tools is also a way of further understanding the wind speed development in this region. An example of such a tool is the the satellite Aeolus by the European Space Agency that was developed and launched in 2018 for the purpose of measuring the global wind profiles from near surface levels up to a 30 km altitude using the Doppler effect. This gives better coverage in terms of wind speed observation over the globe, including remote regions, and the information acquired has improved the quality of global weather forecasts as it gives better starting conditions in regions where measurements are missing (Žagar et al. (2021)). Using such tools to trace wind speed changes provides additional information that is beneficial to not only understand the changes in wind speed and wind power potential for a certain region but to climate change as well.

4.2 Further studies regarding land cover changes

As seen in Eq. 2 in Section 1.1, wind speed is impacted by the pressure gradient force and surface roughness. In this study, the impact of land cover change is not analyzed but this could possibly explain the minor increase in wind speeds since 1959 in ERA5 (see Fig. 9). As Zeng et al., 2019 argues, the stilling and reversal of the mean wind speeds observed in the northern hemisphere were less likely to be due to land-use changes, as the reversal of near-surface wind speed was drastic and land-use changes was not a sudden occurrence for these regions at that particular time. But when looking at ERA5 within the Greater Horn of Africa, the decennial mean wind speed increase could be considered increasing non-drastically. Additionally, parts of the Greater Horn of Africa is developing fast (IEA (2022)), which could mean drastic land cover changes during the recent decades. For these reasons, land cover changes as a possible reason for the increasing wind speed (according to ERA5) in the Greater Horn of Africa cannot be dismissed without further analysis.

4.3 Highest wind power potential in northern Kenya and Somalia

Despite the rather low wind power potential in most of the study region, some minor areas of higher potential were detected in the current climate state and under global warming. The areas that remain with the highest WPD, even under global warming, were around northern Kenya and Somalia (see Fig.18). The potential reasons to why there is a higher WPD these regions are explained in section 4.3.1 and 4.3.2 by a cross equatorial flow that develops to become the so-called Somali low-level jet and the Turkana low-level jet, which could be a branch of the Somali jet due to the topography in the study region.

4.3.1 *The Somali Jet*

Shown by Findlater (1969) a low-level jet stream exists in the regions close to western Indian Ocean particularly during boreal summer. This jet is seen to cross the equator from the south/southeast through eastern Kenya, then head towards India from the southwest passing through most of Somalia, reaching the ITCZ in the northern hemisphere. The so-called Somali jet is important for the Indian monsoon (T. N. Krishnamurti and Bhalme (1976)). Shi et al. (2016) showed that that the Somali jet intensity during boreal spring and summer is correlated to the variability of the Antarctic Oscillation during the previous boreal winter through the SST in the southern high and middle latitudes. The existence and intensity of this jet could therefore explain the higher wind power potential over Somalia. The Somali jet could also explain the high correlation of wind speeds and the IOD as Fig. 11 showed for boreal spring and summer as May-July is when the core of the jet is over the Horn of Africa as the studies by T. Krishnamurti and Findlater (1978) and T. N. Krishnamurti and Bhalme (1976) showed. In order to understand how the wind power potential could change over Somalia, further research regarding the Somali jet under global warming is beneficial. It is also important to add that since Somalia is a coastal country, local phenomena such as sea-breeze could also impact the winds but such phenomenon are not researched in this report.

4.3.2 *The Turkana Jet*

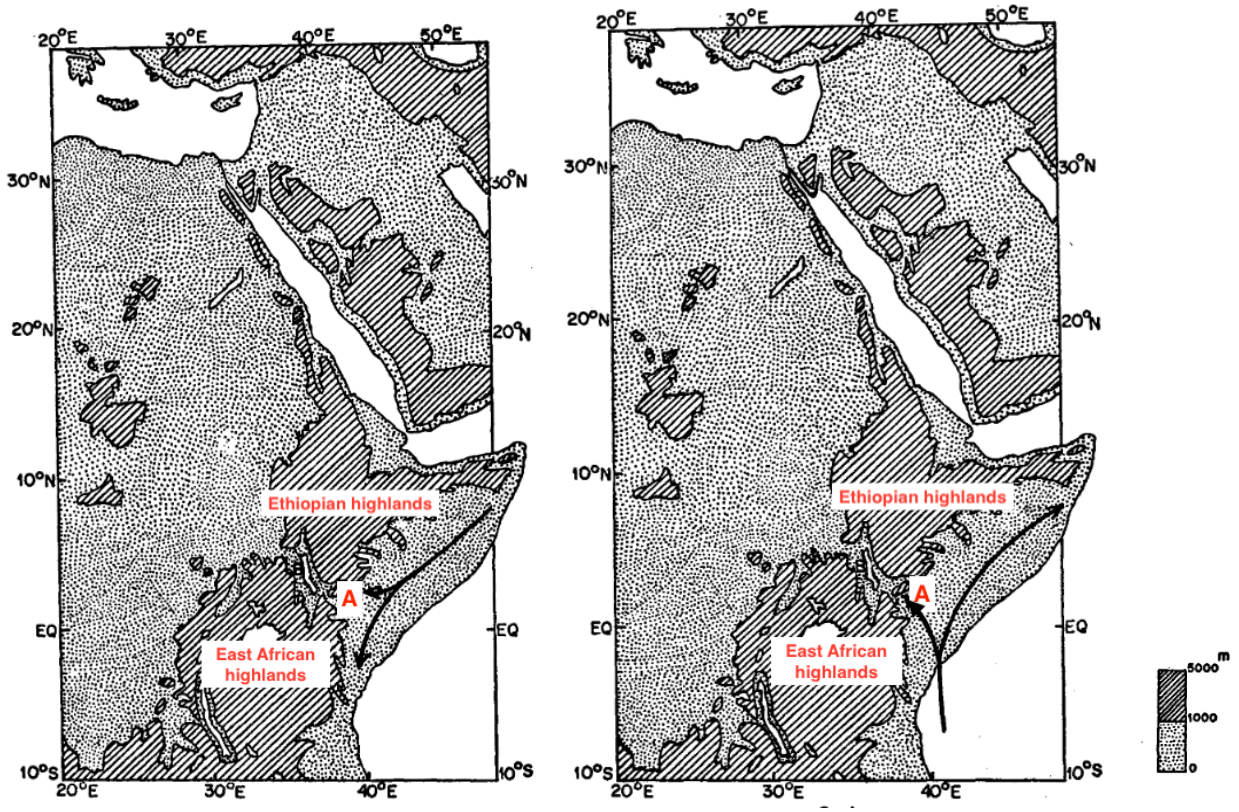

(a) Northeasterly flow during boreal winter (b) Southeasterly flow during boreal summer

Figure 19: A simple illustration of a branch of a flow (black arrows) entering between the Ethiopian highlands and East African highlands at Marsabit, the entrance of the Turkana channel(marked as A) during a) boreal winter and b) boreal summer (J. Kinuthia and Asnani (1982)).

In northern Kenya, a channel is located around the Lake Turkana region with its entrance marked as A in Fig. 19. This channel is a result of the valley between the Ethiopian Highlands where the Simien Mountains are found and the East African highlands where the highest mountains in Africa such as Mount Kenya and Mount Kilimanjaro are found. In this channel, J. Kinuthia and Asnani (1982) and J. H. Kinuthia (1992) showed that there exists a strong low-level jet throughout the year. This could be seen during boreal summer (winter) as south-easterlies (north-easterlies) diverge at the entrance of the channel due to orographic forcing of the Ethiopian and East African highlands. This forces a branch of

the winds to enter the narrow Turkana channel as seen in Fig. 19 and intensify in speed while sustaining the same southeasterly wind direction then slows down once it exists the channel. This phenomenon can be explained by the Venturi effect which is based on the Bernoulli principle. The Turkana low-level jet is most likely the explanation to why the wind power potential is higher in this region. Its occurrence is highly due to the topography, which could also explain why the correlation of the wind speeds and the IOD is close to none in this region as the blue arrow in Fig. 10 showed.

4.4 The Indian Ocean Dipole under global warming

Due to the rather high correlation between the Indian Ocean Dipole and the wind speed over the greater Horn of Africa, understanding how the Indian Ocean could change due to global warming is beneficial knowledge to the future projection of wind speed and the wind power potential. The RCMs in CORDEX-Africa do not tend to completely cover the Indian Ocean and since they are a downscale of GCMs, understanding how the sea surface temperature development is in the GCMs is crucial.

Conway et al. (2007) studied of the behavior of the IOD based on six Global Climate Models show different responses of IOD events under future global warming. 3 of 6 models showed an increasing positive IOD event, 2 showed decreasing positive IOD events and one didn't show a significant change. Zheng et al. (2013) also showed the variability of sea surface temperature among 17 CMIP5 GCMs (including the GCMs mentioned in this study) due to global warming. As seen in Section 3, there is a trend of the IOD going towards the more positive side since 1960s. This is in line with the study by Cai et al. (2009) that showed that there has been less negative IOD events and more positive IOD events which can be explained by the uneven warming rate of the Indian Ocean (slower in the eastern part of the basin than the western part). Cai et al. (2013) also showed that the mean climate conditions under global warming have similar characteristics to the Indian Ocean being in a positive IOD event. The study also showed that the frequency of the IOD events is not projected to change. Furthermore, Cai et al. (2021) also conducted a study simulating moderate and strong positive IOD events under global warming. This resulted in a decrease in moderate positive IOD events and an increase in extreme posit-

ive IOD events. As the wind increase seen in ERA5 is aligned with positive IOD events, a possible increase in the mean wind speed in the future in the Greater Horn of Africa cannot be ruled out. Depending on the magnitude of the increase in wind speeds, the future projections presented in Section 3.3.3 and 3.4 should be investigated further based on the Indian Ocean warming in the GCMs that the RCMs are downscaled from as there could be contradicting outcomes. Further studies regrading the Indian Ocean warming variability is key in determining the future wind power potential for the region.

5 Conclusion

This study shows that there is a small but continuous increase in both 10 m and 100 m wind speeds from ERA5 over the Greater Horn of Africa since 1959 with a significant correlation to the Indian Ocean Dipole. The CORDEX-Africa RCMs do not tend to agree regarding the historical increase in wind speed as they show a more or less constant wind speed development. For the wind power potential in the region, the mean 100 m projected wind speed continued to show a rather constant development for this century on a decennial timescale. While most of the Greater Horn showed a low wind power potential, northern Kenya and Somalia showed distinctive higher wind power potential until the year 2100. This could be explained by the occurance of the low-level Somali jet and Turkana jet.

Despite the non-significant projected changes in the wind speed, there are concerns regarding the historical and initial conditions due to the lack of wind speed observations. Recommendations such as using other parameters like barometric air pressure and remote sensing tools such as satellite are given as away to fill the current (and future) knowledge gap regarding the wind speed in this region. The land cover changes could also be a reason for the small increase, which is recommended to be investigated further as this region is currently rapidly developing. Furthermore, the uncertainties regarding the warming of the Indian Ocean in the future needs more in depth study as the ocean-atmosphere oscillation IOD can be considered to have an impact on the wind speed and the wind power potential in the Greater Horn of Africa.

References

Baudoin, M.-A., & Wolde-Georgis, T. (2015). Disaster risk reduction efforts in the greater horn of africa. *International Journal of Disaster Risk Science*, *6*, 49–61.

Behera, S., Luo, J., Masson, S., Yamagata, T., Delecluse, P., Gualdi, S., & Navarra, A. (2003). Impact of the indian ocean dipole on the east african short rains: A cgcm study. *CLIVAR Exchanges*, *27*(4), 3–5.

Black, E., Slingo, J., & Sperber, K. R. (2003). An observational study of the relationship between excessively strong short rains in coastal east africa and indian ocean sst. *Monthly Weather Review*, *131*(1), 74–94.

Cai, W., Cowan, T., & Sullivan, A. (2009). Recent unprecedented skewness towards positive indian ocean dipole occurrences and its impact on australian rainfall. *Geophysical Research Letters*, *36*(11).

Cai, W., Yang, K., Wu, L., Huang, G., Santoso, A., Ng, B., Wang, G., & Yamagata, T. (2021). Opposite response of strong and moderate positive indian ocean dipole to global warming. *Nature Climate Change*, *11*(1), 27–32.

Cai, W., Zheng, X.-T., Weller, E., Collins, M., Cowan, T., Lengaigne, M., Yu, W., & Yamagata, T. (2013). Projected response of the indian ocean dipole to greenhouse warming. *Nature geoscience*, *6*(12), 999–1007.

Conway, D., Hanson, C., Doherty, R., & Persechino, A. (2007). Gcm simulations of the indian ocean dipole influence on east african rainfall: Present and future. *Geophysical research letters*, *34*(3).

CORDEX. (2022). *Cordex - esgf data availability overview* [Accessed: 2023-02-15]. http://htmlpreview.github.io/?http://is-enes-data.github.io/CORDEX_status.html

Dee, D. P., Uppala, S. M., Simmons, A. J., Berrisford, P., Poli, P., Kobayashi, S., Andrae, U., Balmaseda, M., Balsamo, G., Bauer, d. P., et al. (2011). The era-interim reanalysis: Configuration and performance of the data assimilation system. *Quarterly Journal of the royal meteorological society*, *137*(656), 553–597.

Dunn, R. J. (2019). Hadisd version 3: Monthly updates. *HadISD version 3: monthly updates*.

Dunn, R. J., Willett, K. M., Parker, D. E., & Mitchell, L. (2016). Expanding hadisd: Quality-controlled, sub-daily station data from 1931. *Geoscientific Instrumentation, Methods and Data Systems*, *5*(2), 473–491.

Dunn, R. J., Willett, K. M., Thorne, P. W., Woolley, E. V., Durre, I., Dai, A., Parker, D. E., & Vose, R. (2012). Hadisd: A quality-controlled global synoptic report database for selected variables at long-term stations from 1973–2011. *Climate of the Past*, *8*(5), 1649–1679.

Endris, H. S., Omondi, P., Jain, S., Lennard, C., Hewitson, B., Chang'a, L., Awange, J., Dosio, A., Ketiem, P., Nikulin, G., et al. (2013). Assessment of the performance of cordex regional climate models in simulating east african rainfall. *Journal of Climate*, *26*(21), 8453–8475.

Fiehn, A. (2017). *Transport of very short-lived substances from the indian ocean to the stratosphere through the asian monsoon* (Doctoral dissertation). Christian-Albrechts-Universität Kiel.

Findlater, J. (1969). A major low-level air current near the indian ocean during the northern summer. *Quarterly Journal of the Royal Meteorological Society*, *95*(404), 362–380.

Hersbach, H., Bell, B., Berrisford, P., Hirahara, S., Horányi, A., Muñoz-Sabater, J., Nicolas, J., Peubey, C., Radu, R., Schepers, D., et al. (2020). The era5 global reanalysis. *Quarterly Journal of the Royal Meteorological Society*, *146*(730), 1999–2049.

Holton, J. R., & Hakim, G. J. (2013). *An introduction to dynamic meteorology* (Vol. 88). Academic Press.

IEA. (2022). *Clean energy transitions in the greater horn of africa*. Retrieved September 30, 2022, from https://www.iea.org/reports/clean-energy-transitions-in-the-greater-horn-of-africa

Kinuthia, J., & Asnani, G. (1982). A newly found jet in north kenya (turkana channel). *Monthly Weather Review*, *110*(11), 1722–1728.

Kinuthia, J. H. (1992). Horizontal and vertical structure of the lake turkana jet. *Journal of Applied Meteorology and Climatology*, *31*(11), 1248–1274.

Krishnamurti, T. N., & Bhalme, H. (1976). Oscillations of a monsoon system. part i. observational aspects. *Journal of Atmospheric Sciences*, *33*(10), 1937–1954.

Krishnamurti, T., & Findlater, J. (1978). Observational aspects of the low-level cross-equatorial jet stream of the western indian ocean. *Monsoon dynamics*, 1251–1262.

Libanda, B. (2022). Performance assessment of cordex regional climate models in wind speed simulations over zambia. *Modeling Earth Systems and Environment*, 1–10.

Lu, X., & McElroy, M. B. (2017). Global potential for wind-generated electricity. In *Wind energy engineering* (pp. 51–73). Elsevier.

Lutgens, F. K. (2018). *The atmosphere an introduction to meteorology* (Fourteenth edition).

NOAA. (n.d.). *Dipole mode index (dmi)* [Accessed: 2023-01-17]. https://psl.noaa.gov/gcos_wgsp/Timeseries/DMI/

NOAA. (2020a). *Indian ocean dipole* [Accessed: 2023-05-16]. https://www.climate.gov/media/11095

NOAA. (2020b). *Indian ocean dipole* [Accessed: 2023-05-16]. https://www.climate.gov/media/11097

Ramon, J., Lledó, L., Torralba, V., Soret, A., & Doblas-Reyes, F. J. (2019). What global reanalysis best represents near-surface winds? *Quarterly Journal of the Royal Meteorological Society*, *145*(724), 3236–3251.

Robinson, P., & Henderson-Sellers, A. (2014). *Contemporary climatology*. Routledge.

Saji, N., Goswami, B. N., Vinayachandran, P., & Yamagata, T. (1999). A dipole mode in the tropical indian ocean. *Nature*, *401*(6751), 360–363.

Saji, N., & Yamagata, T. (2003a). Structure of sst and surface wind variability during indian ocean dipole mode events: Coads observations. *Journal of Climate*, *16*(16), 2735–2751.

Saji, N., & Yamagata, T. (2003b). Possible impacts of indian ocean dipole mode events on global climate. *Climate Research*, *25*(2), 151–169.

Sawadogo, W., Reboita, M. S., Faye, A., da Rocha, R. P., Odoulami, R. C., Olusegun, C. F., Adeniyi, M. O., Abiodun, B. J., Sylla, M. B., Diallo, I., et al. (2021). Current and future potential of solar and wind energy over africa using the regcm4 cordex-core ensemble. *Climate Dynamics*, *57*(5-6), 1647–1672.

Schulzweida, U. (2017). Cdo user's guide. *Version 1.4.6*. 1–173.

Shi, W., Xiao, Z., & Xue, J. (2016). Teleconnected influence of the boreal winter antarctic oscillation on the somali jet: Bridging role of sea surface temperature in southern high and middle latitudes. *Advances in Atmospheric Sciences*, *33*, 47–57.

Webster, P. J., Moore, A. M., Loschnigg, J. P., & Leben, R. R. (1999). Coupled ocean–atmosphere dynamics in the indian ocean during 1997–98. *Nature*, *401*(6751), 356–360.

Žagar, N., Rennie, M., & Isaksen, L. (2021). Uncertainties in kelvin waves in ecmwf analyses and forecasts: Insights from aeolus observing system experiments. *Geophysical Research Letters*, *48*(22), e2021GL094716.

Zeng, Z., Ziegler, A. D., Searchinger, T., Yang, L., Chen, A., Ju, K., Piao, S., Li, L. Z., Ciais, P., Chen, D., et al. (2019). A reversal in global terrestrial stilling and its implications for wind energy production. *Nature Climate Change*, *9*(12), 979–985.

Zheng, X.-T., Xie, S.-P., Du, Y., Liu, L., Huang, G., & Liu, Q. (2013). Indian ocean dipole response to global warming in the cmip5 multimodel ensemble. *Journal of Climate*, *26*(16), 6067–6080.